Research Article Vol. 30, No. 16 / 1 Aug 2022 / Optics Express 29833

Optics EXPRESS

5 kHz, 4.2mJ, 900 ps end-pumped Nd:YVO_4 MOPA laser system

YIPING ZHOU,[1] XUDONG LI,[1,3] CHAOJIE WEI,[1] XIAOJIE CHEN,[1] HAOBO XU,[1] RONGWEI FAN,[1] DEYING CHEN,[1] YUGANG JIANG,[2] AND RENPENG YAN[1,*]

[1]*National Key Laboratory of Science and Technology on Tunable Laser, Harbin Institute of Technology, Harbin 150080, China*

[2]*Tianjin Key Laboratory of Optical Thin Film, Tianjin Jinhang Technical Physics Institute, Tianjin 300308, China*

[3]*kevin2025@163.com*

[*]*rpyan@hit.edu.cn*

Abstract: A 5 kHz sub-nanosecond master oscillator power amplifier (MOPA) laser system was reported in this paper. The master oscillator was an electro-optically Q-switched Nd:YVO_4 laser directly pumped at 879 nm, yielding a pulse energy of 520 µJ and a pulse width of 900 ps at 5 kHz. With two Nd:YVO_4 amplifiers directly pumped at 914 nm, the pulse energy was further scaled up. Under the absorbed pump energy of 11.0 mJ, the pulse energy was amplified to 4.2 mJ, corresponding to a peak power of 4.7 MW. The optical-to-optical efficiency of the amplifiers reached 33.5%.

1. Introduction

Pulsed lasers with kHz-level repetition rate, sub-nanosecond pulse width, and mJ-level energy are attractive in many applications, such as lidar [1–3], laser processing [4,5], and nonlinear optics [6,7]. Several methods have been proposed to obtain pulsed laser with sub-nanosecond pulse width, including external modulation [8,9], laser diode (LD) modulation [10,11], and Q-switching technique [12,13].

For the advantage of low cost, simple structure, and high efficiency, Q-switching technique is the most effective approach to producing sub-nanosecond laser pulses. In 2015, S. Han reported a sub-nanosecond passively Q-switched Nd:YVO_4/Cr^{4+}:YAG microchip laser. Laser pulses with a pulse energy of 29 µJ and a pulse width of 897 ps were obtained at 5 kHz [14]. In 2021, Y. Jiang present a kHz-level sub-nanosecond electro-optical Q-switched Nd:YVO_4 laser, yielding a pulse energy of 108 µJ and a pulse width of 919 ps at a repetition rate of 10 kHz [15]. Due to the serious thermal effects under high average power, the pulse energy of Q-switched lasers is limited by the repetition rate [16–18]. The master oscillator power amplifier (MOPA) configuration has been widely employed to extend the pulse energy [19–21]. In 2010 A. Agnesi reported a 10 kHz sub-nanosecond MOPA laser, which consists of a passively Q-switched master oscillator and a double-pass side-pumped Nd:YVO_4 slab amplifier, both pumped with 808 nm LDs. Under the pump energy of 3.84 mJ, the pulse energy was amplified from 60 µJ to 545 µJ [22]. In 2020, W. Wu presented a 1 kHz cavity-dumped sub-nanosecond MOPA laser system. The amplifier was a double-pass side-pumped Nd:YAG amplifier, which was pumped at 808 nm. With a pump energy of 500 mJ, the pulse energy was amplified from 1 mJ to 4.4 mJ [23]. Because the gain of the amplifier strongly depends on the upper-state population density, a high pump density is required to provide a high gain [24]. However, when the repetition rate is above kHz level, the serious thermal effects under high pump density can't be ignored. Therefore, to amplify the pulse energy effectively at kHz repetition rate, the thermal effects in the amplifier also need to be optimized.

#468386 https://doi.org/10.1364/OE.468386
Journal © 2022 Received 21 Jun 2022; revised 20 Jul 2022; accepted 21 Jul 2022; published 29 Jul 2022

$Nd:YVO_4$ crystal presents a high emission cross-section and a polarized emission at 1064 nm, which makes it widely used in Q-switched lasers [25,26]. It has been proved that in-band pumping around 879 nm and 888 nm can reduce the thermal load in $Nd:YVO_4$ effectively [27,28]. Recently, in-band pumping at 914 nm has been proposed, which can further reduce the thermal load [29–31]. By using 914 nm as the pump wavelength instead of the conventional 808 nm, the quantum defect can be reduced from 24.1% to 14.1% [29]. The optical efficiency as high as 78.7% has been achieved in a 914 nm in-band pumped $Nd:YVO_4$ laser [30]. However, because of the small absorption coefficient at 914 nm, a long and highly doped $Nd:YVO_4$ is required to realize a high absorption efficiency [31]. Thus, in-band pumping at 914 nm isn't suitable for the sub-nanosecond oscillator, which needs a short cavity to obtain a short pulse width. But it can be employed in the amplifiers, and there has been no investigation on $Nd:YVO_4$ amplifier in-band pumped at 914 nm. Besides the pump source, it has been proved that the thermal effects can also be reduced obviously by combining an undoped segment with the gain medium and using the multi-segment composite crystal with different doping concentrations [32,33].

In this paper, we demonstrated a sub-nanosecond MOPA laser system, where multi-segment composite $Nd:YVO_4$ crystals and in-band pumping were utilized to reduce the thermal effects. The master oscillator was an electro-optically Q-switched $Nd:YVO_4$ laser directly pumped at 879 nm. Laser pulses with a pulse width of 900 ps and a pulse energy of 520 µJ were obtained at a repetition rate of 5 kHz. Two single-pass amplifiers were used to scale up the pulse energy, with multi-segment composite $Nd:YVO_4$ crystals end-pumped at 914 nm. Under the absorbed pump energy of 11.0 mJ, the pulse energy was amplified to 4.2 mJ, corresponding to a peak power of 4.7 MW. The optical-to-optical efficiency of the amplifiers reached 33.5%. The beam quality factors in the horizontal and vertical directions were $M_x{}^2 = 1.95$ and $M_y{}^2 = 1.87$.

2. Experimental setup

The experimental setup of the sub-nanosecond MOPA laser system is shown in Fig. 1. An LD end-pumped electro-optically Q-switched $Nd:YVO_4$ laser is employed as the master oscillator. The pump source is a fiber-coupled 879 nm LD (LD_1 in Fig. 1, e06.0650879200, nLight, Inc.) with a core diameter of 200 µm, a numerical aperture (N.A.) of 0.22, and a maximum continuous wave (CW) power of 65 W. A pair of aspherical lenses (L_1 and L_2 in Fig. 1) with a coupling ratio of 1:2 is used to re-image the pump light into the gain medium. An a-cut multi-segment composite $Nd:YVO_4$ crystal ($Crystal_1$ in Fig. 1) is employed as the gain medium. The composite crystal contains three parts, whose Nd^{3+} doping concentrations are undoped (2 mm), 0.2 at.% (4 mm) and 0.5 at.% (5 mm), respectively. About 95% of the pump energy is absorbed by the composite crystal. One surface of the composite crystal is coated for high reflection (HR) at 1064 nm and high transmission (HT) at 879 nm. The other surface is coated for HT at 1064 nm. Although $Nd:YVO_4$ is a natural birefringent gain medium with the emission cross-section along the *c* axis higher than that along the *a* axis, radiation with polarization direction along the *a* axis will also oscillate under high gain. To increase the polarization ratio, the end surface of the composite $Nd:YVO_4$ crystal is cut at the Brewster angle. A small size KD_2PO_4 (KD*P) Pockels cell (PKC) is inserted in the cavity as the Q-switch, with a length of 16 mm. Utilizing the birefringence of the KD*P crystal, the propagation direction deviates a little from the optic axis, so that the PKC operates as a quarter-wave plate with no voltage applied to the KD*P crystal, and the Q-switch operated in high-loss mode. When the voltage is increased, the birefringence of the KD*P crystal is compensated for, and the oscillator is switched on. A plane mirror (M_1 in Fig. 1) with a transmission of 80% at 1064 nm is employed as the output coupler. The cavity length of the master oscillator is about 32 mm.

With two plane mirrors (M_2 and M_3 in Fig. 1) the output pulses are guided to the amplifiers. The pump source of the amplifiers is a fiber-coupled 914 nm LD (LD_2 in Fig. 1, e12.1550915105, nLight, Inc.) with a core diameter of 105 µm, an N.A. of 0.22, and a maximum CW power of

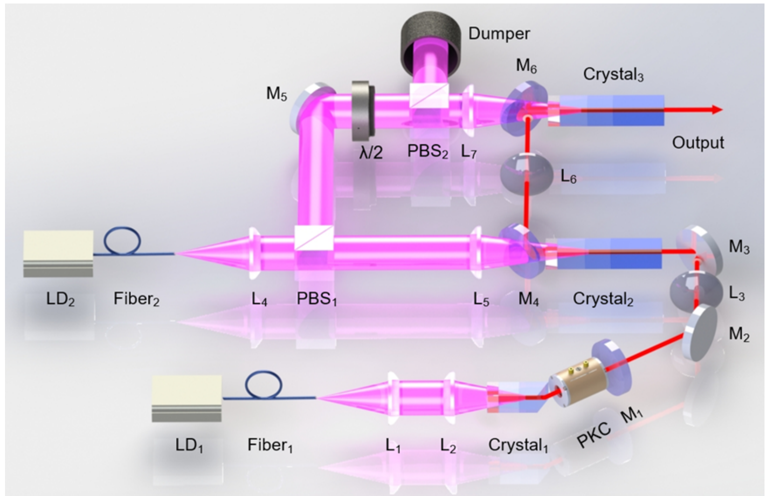

Fig. 1. Experimental setup of the sub-nanosecond MOPA laser system.

155 W. Another pair of aspherical lenses (L_4 and L_5 in Fig. 1) with a coupling ratio of 1:5.2 is used to re-image the pump light into $Crystal_2$. A polarized beam splitter (PBS_1 in Fig. 1) is used to split the pump light and increase the absorption efficiency. A plane mirror (M_5 in Fig. 1) and an aspherical lens (L_7 in Fig. 1) are used to couple the pump light into $Crystal_3$ with a beam diameter of 750 µm. A half-wave plate (λ/2 in Fig. 1) and PBS_2 are used to control the pump energy coupled into $Crystal_3$. The rest pump light is absorbed by a dumper. M_4 and M_6 are two plane mirrors that are coated for HR at 1064 nm and HT at 914 nm at 45°. The beam size of the sub-nanosecond pulses in $Crystal_2$ and $Crystal_3$ are controlled by two convex lenses (L_3 and L_6 in Fig. 1), whose focal lengths are both 150 mm. $Crystal_2$ and $Crystal_3$ are two composite crystals with the same dimension, which consist of a 2-mm-long undoped YVO_4 crystal, an 11-mm-long 1.0-at.%-doped, an 8-mm-long 1.5-at.%-doped, and a 23-mm-long 2.5-at.%-doped Nd:YVO_4 segments. A digital pulse generator is used to control the system timing. Considering the relation between emission lifetime and doping concentration [34], the pump pulse duration of the master oscillator and the amplifiers are set to be 90 µs and 75 µs, respectively. The repetition rate of the laser system is set to be 5 kHz.

3. Results and discussion

Figure 2 shows the pulse energy and pulse width of the sub-nanosecond MOPA laser system. As shown in Fig. 2(a), the pulse width of the Q-switched oscillator decreased with the absorbed pump energy, and finally stabilized at ~900 ps. The output pulse energy of the Q-switched oscillator increased almost linearly with the absorbed pump energy. With the absorbed pump energy of 2.8 mJ, the output pulse energy reached 520 µJ, corresponding to a peak power of 577.8 kW. The optical-to-optical efficiency of the Q-switched oscillator was 18.6% under the maximum pump energy. With the pump energy of the master oscillator further increased, it began to oscillate even in the high-loss mode, due to the high gain and the limited extinction ratio of the PKC. The pulse energy got further amplified by two Nd:YVO_4 amplifiers, which were directly pumped at 914 nm. The Nd:YVO_4 crystal has different absorption coefficients at 914 nm along the two crystallographic axes. With a 1.0-at.%-doped Nd:YVO_4 crystal, the peak absorption coefficients were measured to be 0.51 cm^{-1} along the *c* axis and 0.34 cm^{-1} along the *a* axis. With the polarization direction of the 914 nm pump laser parallel to the *c* axis, the

Optics EXPRESS

absorption efficiency of the composite crystal reached 95%. As shown in Fig. 2(b), when the absorbed pump energy of the amplifiers was 11.0 mJ, the output pulse energy reached 4.2 mJ, corresponding to a peak power of 4.7 MW. The optical-to-optical efficiency of the amplifiers reached 33.5%. Because of the utilization of direct pumping at 914 nm, the relatively high pulse energy of the seed laser, and the good mode matching in the end-pumping structure, the optical-to-optical efficiency was obviously higher than our previous work [17,23,35,36].

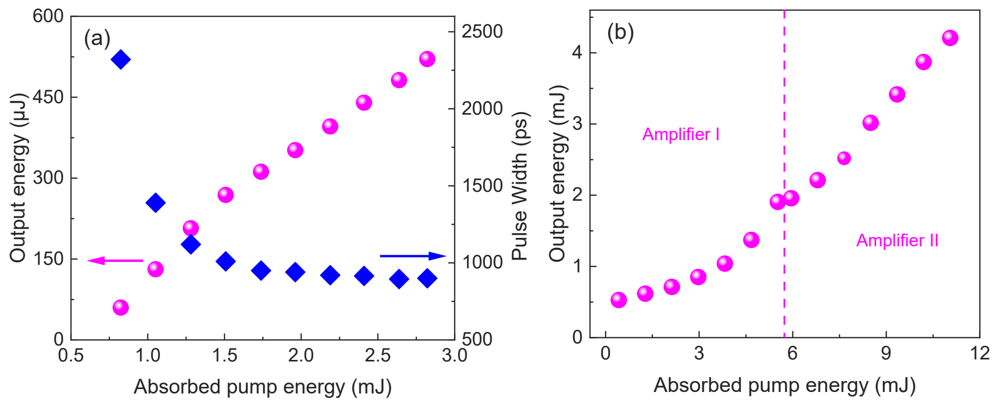

Fig. 2. Pulse energy and pulse width of the sub-nanosecond MOPA laser system. (a) Pulse energy and pulse width of the master oscillator versus the absorbed pump energy, (b) pulse energy of the amplifiers versus the absorbed pump energy.

Besides the cavity length, the output pulse width of the electro-optically Q-switched laser also strongly depends on the rising time of the PKC driver. In order to achieve the sub-nanosecond pulse width, a high-speed voltage driver was used in this experiment. The temporal profile of the high voltage output from the driver was measured with a high voltage probe (THDP0100, Tektronix Inc. bandwidth: 100 MHz) and a digital oscilloscope (DPO7104, Tektronix Inc. bandwidth: 1 GHz). As shown in Fig. 3(a), the driver provided a voltage of 3.6 kV with a rising front of less than 10 ns. With a fast photodiode (ET-3500, Electro-Optics Technology Inc. rising time: 25 ps) and the digital oscilloscope, the pulse characters of the MOPA laser system were measured. The pulse width kept almost constant at 900 ps during the amplification process, and the single pulse profile is shown in Fig. 3(b). No satellite pulse was observed after the main pulse. Thus, the piezoelectric ringing phenomenon wasn't obvious in the PKC, which is the main factor that limits the operations at high repetition rates. It is caused by acoustic waves inside the crystal, which are induced by the high voltage pulses applied to the PKC. Acoustic waves cause modification of the refractive index of the crystal and reduce the extinction ratio of the PKC. It has been found that the piezoelectric ringing is related to the size of PKC, and small size is beneficial for reducing the piezoelectric ringing [37]. Therefore, the small size PKC used in this experiment can not only reduce the cavity length but also avoid the piezoelectric ringing phenomenon. The pulse width can be further shortened by using a PKC driver with faster rising time. But limited by the cavity length, the shortest pulse width was still at hundreds of picoseconds level. The temporal pulse trains of the master oscillator and the amplifiers are shown in Fig. 3(c) and Fig. 3(d), respectively, which presented good amplitude stability. The corresponding coefficients of variation (CV, the ratio of the standard deviation to the mean) were calculated to be 2.77% and 1.94%, respectively.

By using the traveling knife-edge method, the beam radius variations of the sub-nanosecond MOPA laser system were measured, as shown in Fig. 4. The beam quality factors of the master oscillator in the two orthogonal directions were calculated to be $M_x^2 = 1.54$ and $M_y^2 = 1.42$ at the maximum output energy. The spherical aberration was serious in the small size gain medium

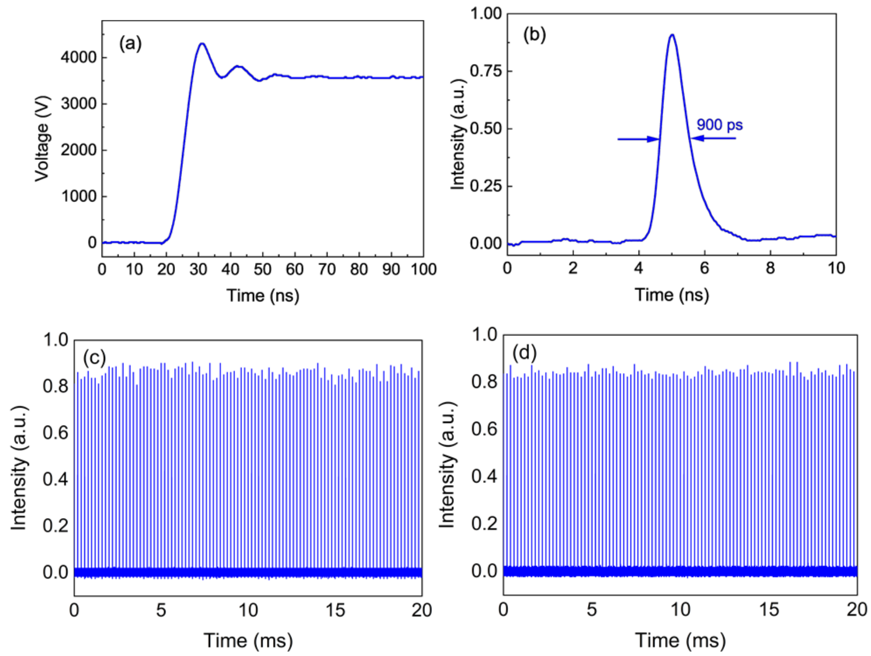

Fig. 3. Waveform profiles of the sub-nanosecond MOPA laser system at the maximum output energy. (a) Temporal profile of the high voltage output from the PKC driver, (b) temporal profile of the single pulse, (c) pulse train of the master oscillator, (d) pulse train of the amplifiers.

under high pump power and caused the beam quality factors in the master oscillator to deteriorate. After passing the two amplifiers, the beam quality factors in the two orthogonal directions became $M_x^2 = 1.95$ and $M_y^2 = 1.87$. The good mode matching and heat management in the amplifiers helped prevent the beam quality factors from getting worse heavily under the high average pump power.

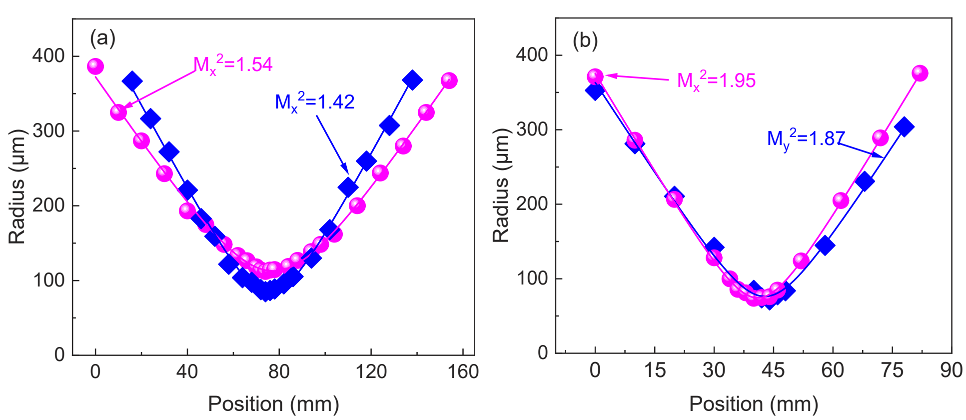

Fig. 4. Beam radius variations of the sub-nanosecond MOPA laser system at the maximum output energy. (a) Outputs from the master oscillator, (b) outputs from the amplifiers.

The spatial beam distributions of the sub-nanosecond MOPA laser system were measured by a laser beam analyzer (LBA-712PC-D, Spiricon Inc.). As shown in Fig. 5(a) and Fig. 5(b), the beam profiles of the master oscillator had a larger size in the horizontal direction, which was induced by the cutting angle of the gain medium. After being amplified by the two amplifiers, the laser beam profiles became more symmetry in the horizontal and vertical directions.

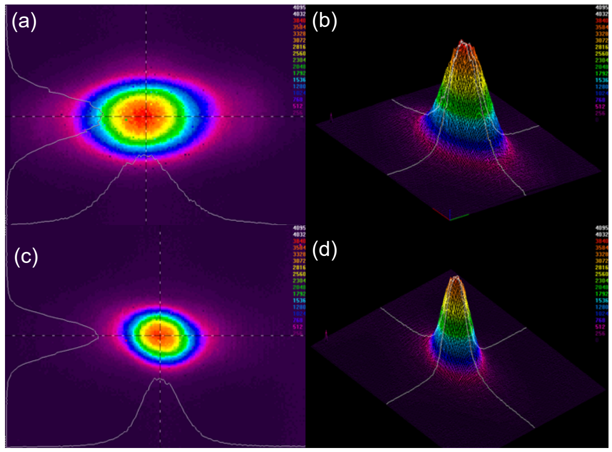

Fig. 5. Laser beam profiles of the sub-nanosecond MOPA laser system at the maximum output energy. (a) Outputs from the master oscillator in two dimensions, (b) outputs from the master oscillator in three dimensions, (c) outputs from the amplifiers in two dimensions, (d) outputs from the amplifiers in three dimensions.

By utilizing a focusing lens with a focal length of 17 mm, the air-breakdown spark was generated by the sub-nanosecond laser, as shown in Fig. 6. It showed the potential of this sub-nanosecond MOPA laser system in the application of laser diagnostics, where high peak power and high repetition rate are required.

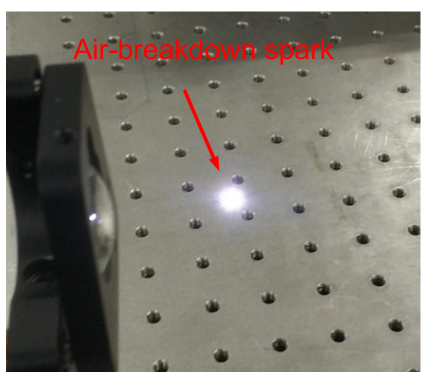

Fig. 6. The air-breakdown spark generated by the sub-nanosecond laser.

4. Conclusion

In this paper, a 5 kHz sub-nanosecond MOPA laser system was developed. To reduce the thermal effects, multi-segment composite Nd:YVO_4 crystals with different doping concentrations and in-band pumping were utilized in the laser system. An electro-optically Q-switched Nd:YVO_4

Optics EXPRESS

laser directly pumped at 879 nm was employed as the master oscillator, generating laser pulses with a pulse energy of 520 µJ and a pulse width of 900 ps. Two end-pumped amplifiers directly pumped at 914 nm were used to further extend the pulse energy. With a pump energy of 11.0 mJ, the pulse energy was amplified to 4.2 mJ, corresponding to a peak power of 4.7 MW. The optical-to-optical efficiency of the amplifiers reached 33.5%. The beam quality factors in the horizontal and vertical directions were ${M_x}^2 = 1.95$ and ${M_y}^2 = 1.87$, respectively. With a focusing lens, the air-breakdown spark was generated by the laser pulses. This 5 kHz sub-nanosecond MOPA laser system is a promising laser source for many applications including lidar and laser diagnostics. This research shows that the Nd:YVO_4 amplifier directly pumped at 914 nm is suitable for amplifying 1064 nm laser pulses.

Funding. National Natural Science Foundation of China (61605032, 61705165, 61775167, 61975150); Natural Science Foundation of Tianjin City (18JCZDJC37900, 19JCZDJC38400).

Disclosures. The authors declare no conflicts of interest.

Data availability. Data underlying the results presented in this paper are not publicly available at this time but may be obtained from the authors upon reasonable request.

References

1. A. Swatantran, H. Tang, T. Barrett, P. Decola, and R. Dubayah, "Rapid, high-resolution forest structure and terrain mapping over large areas using single photon lidar," Sci. Rep. **6**(1), 28277 (2016).
2. Z. P. Li, X. Huang, Y. Cao, B. Wang, Y. H. Li, W. Jin, C. Yu, J. Zhang, Q. Zhang, C. Z. Peng, F. Xu, and J. W. Pan, "Single-photon computational 3D imaging at 45 km," Photonics Res. **8**(9), 1532–1540 (2019).
3. J. J. Degnan, "Scanning, multibeam, single photon lidars for rapid, large scale, high resolution, topographic and bathymetric mapping," Remote Sens. **8**(11), 958 (2016).
4. P. Kubis, J. Winter, A. Gavrilova, M. Hennel, S. Schlosser, I. Richter, A. Distler, M. Heyder, S. Kery, P. Lenk, S. Geiger, C. J. Brabec, H. P. Huber, and H. J. Egelhaaf, "All sub-nanosecond laser monolithic interconnection of OPV modules," Prog. Photovoltaics Res. Appl. **27**(6), 479–490 (2019).
5. B. Heise, S. E. Schausberger, S. Häuser, B. Plank, D. Salaberger, E. Leiss-Holzinger, and D. Stifter, "Full-field optical coherence microscopy with a sub-nanosecond supercontinuum light source for material research," Opt. Fiber chnol. **18**(5), 403–410 (2012).
6. S. Hayashi, T. Shibuya, H. Sakai, T. Taira, C. Otani, Y. Ogawa, and K. Kawase, "Tunability enhancement of a terahertz-wave parametric generator pumped by a microchip Nd:YAG laser," Appl. Opt. **48**(15), 2899–2902 (2009).
7. R. Bhandari, N. Tsuji, T. Suzuki, M. Nishifuji, and T. Taira, "Efficient second to ninth harmonic generation using megawatt peak power microchip laser," Opt. Express **21**(23), 28849–28855 (2013).
8. R. A. Meijer, A. S. Stodolna, K. S. E. Eikema, and S. Witte, "High-energy Nd:YAG laser system with arbitrary sub-nanosecond pulse shaping capability," Opt. Lett. **42**(14), 2758–2761 (2017).
9. M. Nie, Q. Liu, E. Ji, X. Cao, X. Fu, and M. Gong, "Active pulse shaping for end-pumped Nd:YVO_4 amplifier with high gain," Opt. Lett. **42**(6), 1051–1054 (2017).
10. X. Wang, B. Wang, J. Wang, and W. Cheng, "Compact sub-nanosecond pulse seed source with diode laser driven by a high-speed circuit," Opt. Commun. **416**, 84–88 (2018).
11. J. Huikari, E. Avrutin, B. Ryvkin, and J. Kostamovaara, "High-energy sub-nanosecond optical pulse generation with a semiconductor laser diode for pulsed TOF laser ranging utilizing the single photon detection approach," Opt. Rev. **23**(3), 522–528 (2016).
12. N. Pavel, M. Tsunekane, and T. Taira, "Nd:YAG/Cr^{4+}:YAG monolithic micro-laser with multiple-beam output for engine ignition," Opt. Express **19**(10), 9378 (2011).
13. H. C. Lee, D. W. Chang, E. J. Lee, and H. W. Yoon, "High-energy, sub-nanosecond linearly polarized passively Q-switched MOPA laser system," Opt. Laser Technol. **95**, 81–85 (2017).
14. S. Han, Y. Liu, F. Zhang, H. Yu, Z. Wang, Q. Gu, and X. Xu, "Sub-nanosecond passively Q-switched Nd:YVO_4/Cr^{4+}:YAG microchip lasers," Infrared Phys. Technol. **68**, 197–200 (2015).
15. Y. Jiang, P. Li, X. Fu, and Q. Liu, "Sub-nanosecond, single longitudinal mode laser based on a VBG-coupled EOQ Nd:YVO_4 oscillator for remote sensing," Microw. Opt. Technol. Lett. **63**(10), 2541–2547 (2021).
16. Y. He, Y. Ma, J. Li, X. Li, R. Yan, J. Gao, X. Yu, R. Sun, and Y. Pan, "Continuous-wave and passively Q-switched 1.06 µm ceramic Nd:YAG laser," Opt. Laser Technol. **81**, 46–49 (2016).
17. Y. Zhou, X. Li, W. Wu, Y. Jiang, R. Fan, D. Chen, and R. Yan, "500 Hz, 47.1 mJ, sub-nanosecond MOPA laser system," Opt. Laser Technol. **134**, 106592 (2021).
18. L. Cini and J. I. Mackenzie, "Analytical thermal model for end-pumped solid-state lasers," Appl. Phys. B Lasers Opt. **123**(12), 273 (2017).
19. X. Fu, Q. Liu, X. Yan, J. Cui, and M. Gong, "120 W high repetition rate Nd:YVO_4 MOPA laser with a Nd:YAG cavity-dumped seed laser," Appl. Phys. B Lasers Opt. **95**(1), 63–67 (2009).

Optics EXPRESS

20. Q. Liu, H. Chen, X. Yan, and M. Gong, "36.5 W high beam quality 532 nm green laser based on dual-rod AO Q-switched resonator," Opt. Commun. **284**(13), 3383–3386 (2011).
21. T. Kawasaki, V. Yahia, and T. Taira, "100 Hz operation in 10 PW/sr·cm^2 class Nd:YAG Micro-MOPA," Opt. Express **27**(14), 19555–19561 (2019).
22. A. Agnesi, P. Dallocchio, F. Pirzio, and G. Reali, "Sub-nanosecond single-frequency 10-kHz diode-pumped MOPA laser," Appl. Phys. B Lasers Opt. **98**(4), 737–741 (2010).
23. W. Wu, X. Li, R. Yan, D. Chen, and Y. Jiang, "Low heat-effect side-pumping gain module with evenly Gaussian to flat-top fluorescence distribution," Opt. Laser Technol. **127**, 106203 (2020).
24. J. M. Eggleston, L. M. Frantz, and H. Injeyan, "Deviation of the Frantz-Nodvik equation for zig-zag optical path, slab geometry laser amplifiers," IEEE J. Quantum Electron. **25**(8), 1855–1862 (1989).
25. Y. Jiang, M. Nie, R. Guo, X. Fu, and Q. Liu, "Pushing the limit of pulse duration in Q-switched solid-state lasers with high gain," Opt. Laser Technol. **129**, 106276 (2020).
26. J. Gao, X. Yu, B. Wei, and X. D. Wu, "Quasi-three-level Nd:YVO_4 laser operation at 914 nm under 879 nm diode laser pumping," Laser Phys. **20**(7), 1590–1593 (2010).
27. Q. Liu, M. Nie, F. Lu, and M. Gong, "High-Power, Wavelength-Locked 878.6 nm In-Band Pumped, Acoustic-Optically Q-Switched Nd:YVO_4 MOPA Laser with TEM_{00} Mode," IEEE Photonics J. **8**(4), 1502309 (2016).
28. L. Mc Donagh and R. Wallenstein, "Low-noise 62W CW intracavity-doubled TEM_{00} Nd:YVO_4 green laser pumped at 888 nm," Opt. Lett. **32**(7), 802–804 (2007).
29. T. Waritanant and A. Major, "Thermal lensing in Nd:YVO_4 laser with in-band pumping at 914 nm," Appl. Phys. B Lasers Opt. **122**(5), 135 (2016).
30. D. Sangla, M. Castaing, F. Balembois, and P. Georges, "Highly efficient Nd: YVO4 laser by direct in-band diode pumping at 914 nm," Opt. Lett. **34**(14), 2159–2161 (2009).
31. L. Chang, C. Yang, X. J. Yi, Q. K. Ai, L. Y. Chen, M. Chen, G. Li, J. H. Yang, and Y. F. Ma, "914 nm LD end-pumped 31.8 W high beam quality E-O Q-switched Nd:YVO_4 laser without intracavity polarizer," Laser Phys. **22**(9), 1369–1372 (2012).
32. A. M. Rodin, M. Grishin, and A. Michailovas, "Picosecond laser with 11 W output power at 1342 nm based on composite multiple doping level Nd:YVO_4 crystal," Opt. Laser Technol. **76**, 46–52 (2016).
33. S. Li, G. Li, S. Zhao, and X. Wang, "Theoretical and experimental study on high peak power sub-nanosecond pulse characteristics of multi-segment composite Nd:YVO_4 laser," IEEE J. Quantum Electron. **51**(11), 1700708 (2015).
34. Y. F. Chen, L. J. Lee, T. M. Huang, and C. L. Wang, "Study of high-power diode-end-pumped Nd:YVO_4 laser at 1.34 µm: Influence of Auger upconversion," Opt. Commun. **163**(4-6), 198–202 (1999).
35. W. Wu, X. Li, R. Yan, D. Chen, and S. Tang, "Cavity-dumped burst-mode Nd:YAG laser master-oscillator power-amplifier system with a flat-top beam output realized by gain profile-controlled side pumping," Opt. Express **30**(12), 20401–20414 (2022).
36. Y. Zhou, X. Li, H. Xu, R. Yan, Y. Jiang, R. Fan, and D. Chen, "High-pulse-energy passively Q-switched sub-nanosecond MOPA laser system operating at kHz level," Opt. Express **29**(11), 17201–17214 (2021).
37. J. Shang, J. Sun, Q. Li, J. Wu, L. Zhang, F. Dou, C. Dong, and J. Xu, "High-repetition-rate $LiNbO_3$ electro-optic Q-switched Nd:YVO_4 laser," Acta Opt. Sin. **47**(5), 514001 (2018).